

## Geophysical investigation of the Honningsvåg igneous complex, Scandinavian Caledonides

T. H. TORSVIK<sup>1</sup>, O. OLESEN<sup>1</sup>, A. TRENCH<sup>1,4</sup>, T. B. ANDERSEN<sup>2</sup>,  
H. J. WALDERHAUG<sup>3</sup> & M. A. SMETHURST<sup>1</sup>

<sup>1</sup>*Geological Survey of Norway, PB 3006 Lade N-7002 Trondheim, Norway*

<sup>2</sup>*Institute of Geology, University of Oslo, PB 1047 0316 Blindern, Oslo 3, Norway*

<sup>3</sup>*Institute of Solid Earth Geophysics, University of Bergen N-5014 Bergen, Norway*

<sup>4</sup>*Present address: Department of Geology, University of Western Australia, Nedlands, Perth, 6009, Australia*

**Abstract:** The Honningsvåg igneous complex within the Magerøy nappe, northern Norway, has marked magnetic and gravimetric signatures. Palaeomagnetic studies reveal a Siluro-Devonian (Scandian) dual-polarity remanence (NE and up—SW and down; mean declination =  $-38^\circ$  and  $\alpha_{95} = 8.4^\circ$ ). Rock-magnetic and petrological studies indicate a pure magnetite host for the remanent magnetization component. Magnetic-fabric ellipsoids delineate D1 and D2 Scandian structures affecting the area, and demonstrate an internal reclined fold-structure of the Honningsvåg igneous complex. Forward-modelling demonstrates that a short-wavelength, positive aeromagnetic anomaly (*c.* 700 nT) over the northwestern part of the complex is associated with an area of reverse remanent polarity (SW and down). Conversely, areas of normal remanence polarity (NE and up most common) are associated with magnetic 'lows' or 'quiet' zones. The gravity field in the vicinity of the complex displays a symmetrical positive anomaly of approximately 200 g.u. (wavelength 15 km). This can be attributed to a density contrast of approximately 0.20 Mg/m<sup>3</sup> between the gabbros of the Honningsvåg complex (2.93) and surrounding metasediments (2.73). An optimal geophysical and geological model demonstrates that the complex has been tilted through  $90^\circ$ , and now has the form of a steeply dipping reclined fold-structure extending to a depth of at least 6 km.

Palaeomagnetic remanence acquisition post-dates emplacement of the Magerøy nappe (late D1), and probably originated during post-D1 uplift. Brittle, upper-crust, D2 deformation which continued into Devonian times, folded the Honningsvåg igneous complex and introduced a small but systematic dispersion in the palaeomagnetic remanence directions. The magnetization is, therefore, post-D1 but pre-D2 in age, and can be termed 'syn-Scandian'. Palaeomagnetic and isotopic evidence suggests a syn-tectonic magnetization age of *c.* 410 Ma. The palaeomagnetic pole ( $N7^\circ$  and  $E344^\circ$ ) resembles that from the underlying Kalak nappe complex. It is therefore inferred that the Scandian emplacement of the Magerøy nappe was synchronous with a thermal event which affected the older and underlying Finnmarkian-deformed Kalak nappe complex.

Palaeomagnetic remanence studies have proved valuable in dating rock formations and tectonothermal events, elucidating regional tectonic problems and constraining palaeogeographic scenarios. Conversely, the anisotropy of magnetic susceptibility, or anisotropy of remanence, can be used to image a rock's micro-fabric and identifying lineations or foliations, primary or tectonic, not otherwise detected megascopically in the field. Magnetic fabric and remanence signature are often unrelated; thus a rock may show primary fabrics whereas remanence can be reset during later thermal events. In this respect, a change in the orientation of the magnetic fabric ellipsoids might require recrystallization, whereas remanence can be completely or partially 'reset' at moderate temperatures without appreciable recrystallization.

Anisotropy of remanence studies are important when analysing thermally induced remanent magnetizations (TRM) in an anisotropic rock, a situation often found in uplifted metamorphic terranes. In areas with diverse fabric patterns, TRM directions would be expected to be deflected from the ambient field direction, resulting in an increased dispersal of remanence directions. Thus, anisotropy of remanence studies might enable the adjustment of TRM directions such that the deflection caused by magnetic anisotropy can be reversed.

Conversely, aeromagnetic and gravity data offer important constraints on basement structures, fault patterns, and depths to anomaly sources. The interpretation of potential field data is constrained by density, remanence and susceptibility measurements made on rock samples collected in the region of study; hence precise, quantitative, analysis of aeromagnetic and gravity anomalies requires a good petrophysical database. In this account the geophysical methods outlined above are combined to provide a better understanding of the Honningsvåg igneous complex from the island of Magerøy in the Caledonides of northern Norway.

### Geological setting

The Honningsvåg igneous complex near North Cape constitutes an important element of the Magerøy Nappe (Fig. 1) which, together with the minor Skarsvåg nappe, is the highest unit in the Caledonian tectonostratigraphy of northernmost Norway (Andersen 1981; Roberts & Andersen 1985). Over the last two decades, emplacement of nappes in this region of the Caledonides has been considered to relate to two separate orogenic events; the lower Gaissa, Laksefjord and Kalak nappe complexes (Fig. 1) were thought to have been initially

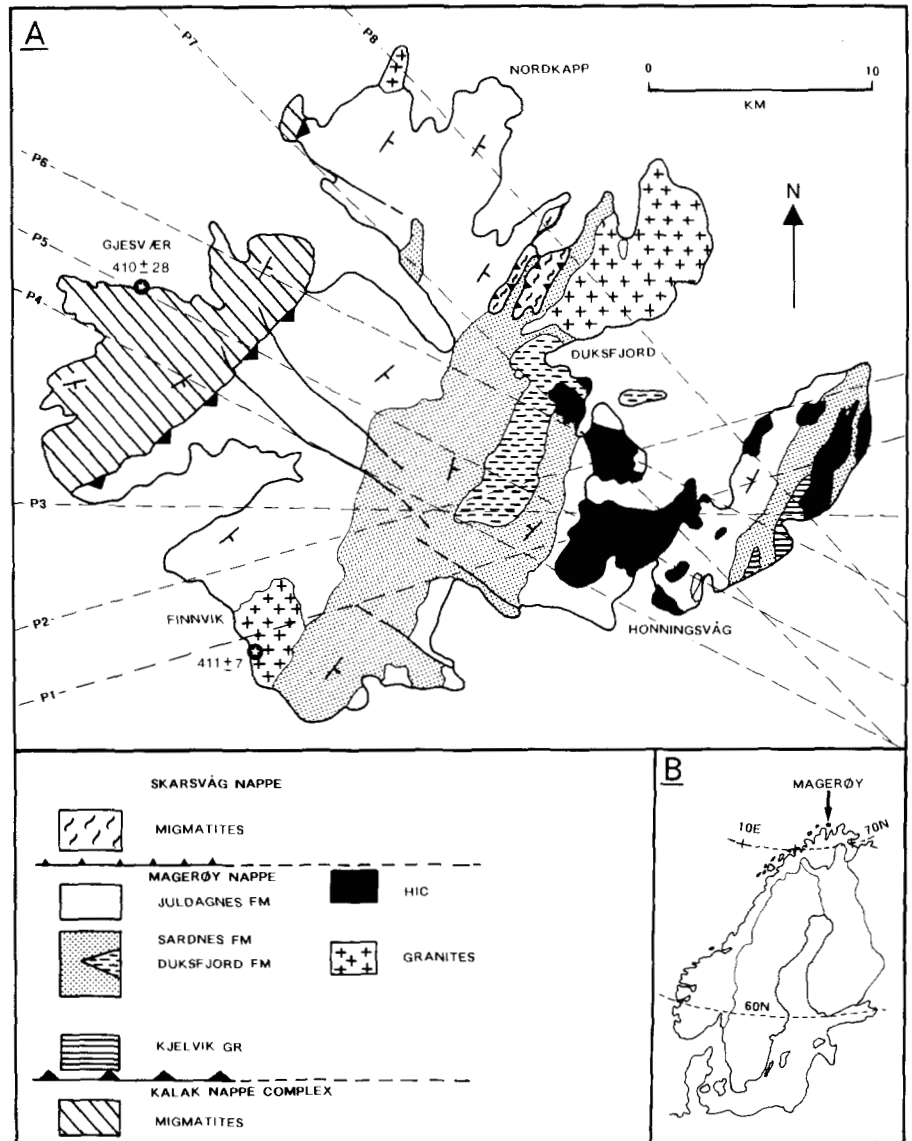


**Fig. 1.** (A) Geological sketch map of Magerøy (after Andersen 1981; Roberts & Andersen 1985). Dashed lines P1–P8 refer to gravimetric, aeromagnetic & topographic lines. The geographic location of the Gjesvær migmatites ( $410 \pm 28$  Ma, Rb–Sr whole rocks; Andersen *et al.* 1982) and the syn-orogenic (Scandian) Finnvik Granite ( $411 \pm 7$ , Rb–Sr whole rock; Andersen *et al.* 1982) are shown. (B) Map of Scandinavia showing the location of Magerøy. HIC, Honningsvåg igneous complex.

emplaced in a Late Cambrian–Early Ordovician Finnmarkian phase (Sturt *et al.* 1978), while the upper units, including the Magerøy Nappe, were emplaced solely during the Late Silurian–Early Devonian Scandian event (Ramsay & Sturt 1976; Andersen *et al.* 1982). In recent years, accumulating radiometric evidence concerning the tectonothermal and magmatic evolution of rocks from the Kalak Nappe Complex has shown that the original definition of the ‘Finnmarkian’ as a major phase of nappe translation (Sturt *et al.* 1975) required critical reconsideration (Pedersen *et al.* 1989; Aitchison *et al.* 1989; Daly *et al.* 1991).

The Honningsvåg igneous complex (Curry 1975; Robins *et al.* 1987) is intrusive into the rocks of the Magerøy nappe. These include an approximately 5.5 km thick sequence of metasediments and syn-orogenic granites in addition to the mafic/ultramafic Honningsvåg igneous complex. The Magerøy Nappe lithologies underwent polyphase deformation and greenschist to amphibolite facies metamorphism during nappe emplacement in the Silurian–Early Devonian Scandian phase (Andersen 1981; Andersen *et al.* 1982). The tectonothermal

Scandian event also affected the underlying Kalak lithologies (Andersen *et al.* 1982; Dallmeyer 1988; Torsvik *et al.* 1990, 1991) that are separated from the Magerøy Nappe by a thick package of amphibolite facies mylonites (Ramsay & Sturt 1976). The metasedimentary rocks of the Magerøy Nappe were deformed in large-scale, north-plunging, overturned to recumbent folds during nappe emplacement. Deformation also affected the syn-kinematic (D1–D2) intrusions of the Honningsvåg igneous complex (Andersen 1981; Roberts & Andersen 1985). The subsequent D2 phase was characterized by open to closed, upright to slightly overturned folds in retrograde greenschist facies metamorphism (Andersen 1981). The complex comprises a series of layered ultramafic/mafic intrusions, traditionally regarded as a syn-orogenic Scandian complex, since it allegedly intrudes fossiliferous Llandoveryan metasediments within the Magerøy nappe (Curry 1975, Andersen 1981, Roberts & Andersen 1985, Robins *et al.* 1987). Recently, overlapping Sm–Nd and Rb–Sr mineral whole-rock dates (558–468 Ma) reported from the Honningsvåg igneous complex have cast some doubt on this intrusive relationship and on

the assumed Silurian age of the complex (Krill *et al.* 1989), but satisfactory geological observations to support these ages and refute the previous interpretation of an intrusive relationship between the Honningsvåg igneous complex and the fossiliferous rocks are still not available (Andersen 1989) as the complex appears to truncate early-Scandian D1 structures (Andersen 1981; Roberts & Andersen 1985). We shall return to this problem below in discussing the palaeomagnetic data. The cumulate layering of the Honningsvåg igneous complex defines a reclined fold, which has been explained either as relating to sub-horizontal D2 shortening, or as a primary basin-shaped magma chamber feature (Robins *et al.* 1987).

117 drill-cores (250 specimens) from 10 sites were sampled for palaeomagnetic/physical purposes (Figs 1A & 2). Sampling included intrusive megabreccias (site 2) and cumulates of peridotite (sites 1 & 3), troctolite/olivine gabbro (sites 4–8) and gabbro/gabbro–norite (sites 9 & 10).

### Palaeomagnetic experiments

Measurements of natural remanent magnetization (NRM) of core samples were made with a two-axis cryogenic and a spinner magnetometer. Within-site NRM directions are well grouped (Table 1) and apart from results from sites 2 and 6 (reverse palaeomagnetic polarity, SW and down) they are also well grouped at a site level (normal palaeomagnetic polarity, NE and up; see regional polarity distribution in Fig. 2).

**Table 1.** Natural remanent magnetization site-means and bulk-susceptibility

Site	P	Dec	Inc	$\alpha_{95}$	Nr	Int	Ns	Sus
1	N	026	-28	4.5	23	2699 ± 2000	6	1087(1063) ± 237
2	R	215	+57	6.1	14	566 ± 162	5	10441(10328) ± 1719
3	N	043	-30	7.4	13	21 ± 5	7	460(455) ± 78
4	N	048	-4	14.2	17	219 ± 206	5	1860(1840) ± 298
5	N	061	-47	13.6	28	967 ± 783	8	4076(2812) ± 2626
6	R	247	+65	29.3	15	89 ± 63	6	2196(2080) ± 889
7	N	079	-63	26.4	13	201 ± 99	6	7582(7345) ± 2112
8	N	051	-10	8.6	24	342 ± 218	8	4334(4086) ± 1641
9	N	032	-12	14.0	22	979 ± 1252	8	2587(2360) ± 1268
10	N	070	-11	24.9	15	71 ± 47	6	3198(2704) ± 1692
<i>Normal Polarity Average</i>								
		049	-26	18.1	8*	687 ± 895	8*	3148(2380) ± 2248

Dec = mean declination; Inc, mean inclination; P, palaeomagnetic polarity; Nr, number of specimens measured for remanence (sites\*); Ns, number of specimens measured for susceptibility (sites\*);  $\alpha_{95}$ , 95% confidence circle; Int, NRM intensity in mA/m; Sus, bulk volume susceptibility in  $10^{-6}$  SI units (logarithmic means are shown in parentheses).

Mean declination, inclination and  $\alpha_{95}$  are calculated using Fisher (1953) statistics. Int and Sus values are given as arithmetic means with the (±) range of one standard deviation.

Mean geographic sampling location: N71–E026°.

170 specimens were stepwise demagnetized utilizing both thermal and alternating field (AF) demagnetization methods. Characteristic remanence components were calculated by least square analysis. The demagnetization results are of excellent quality (Fig. 3) and can be summarized as follows.

(1) Single-component high-unblocking components ( $T_b < 580^\circ\text{C}$ ), denoted **H**, depict *normal* polarity palaeomagnetic magnetizations (NE, up; Fig. 3A & B). Directional stability commonly exceeds the maximum available AF field of 95 mT (Fig. 3B). Antipodal *reverse* polarity directions (SW, down) were observed at sites 2 and 6 (Figs 2 & 3C). From site 6, however, characteristic remanence components proved difficult to determine due to viscous behaviour during both thermal and AF demagnetization.

(2) A two-component magnetization structure was occasionally observed (Fig. 3C & D, Table 2), and in such instances the lower unblocking temperature/coercivity component (NNE, down), denoted **L**, is randomized at temperatures/AF fields below 400–510°C/4–30 mT.

### Opaque minerals

Palaeomagnetic and rock-magnetic experiments have identified pseudo- or single-domain magnetite/low-Ti titanomagnetite as the principal magnetic mineral phase for the following reasons (cf. Figs 3 & 4):

- (1) thermomagnetic curves display Curie temperatures near 580°C;
- (2) unblocking temperatures are usually discrete below 580°C;
- (3) high medium destructive AF fields, averaging 50 mT;
- (4) isothermal remanent magnetization (IRM) saturation is achieved in fields of 200–300 mT;
- (5) remanence coercivity forces approximate to 40 mT.

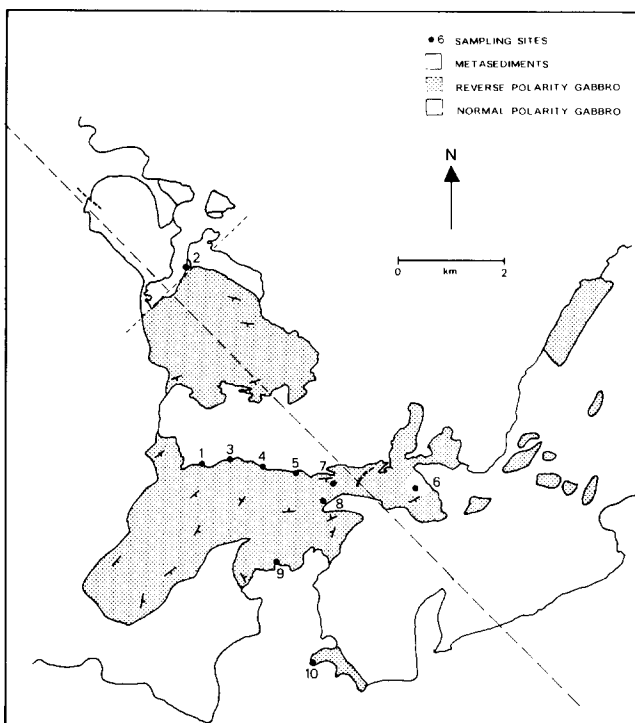


**Fig. 2.** Simplified map of the Honningsvåg igneous complex (after Robins 1990). Numbers refer to palaeomagnetic sampling sites. Areas of normal and reverse palaeomagnetic NRM polarity are tentatively indicated as evidenced from NRM measurements (Table 1) and the aeromagnetic signature/modelling. See Fig. 1A for the geographic location of the Honningsvåg igneous complex within the Magerøy nappe.

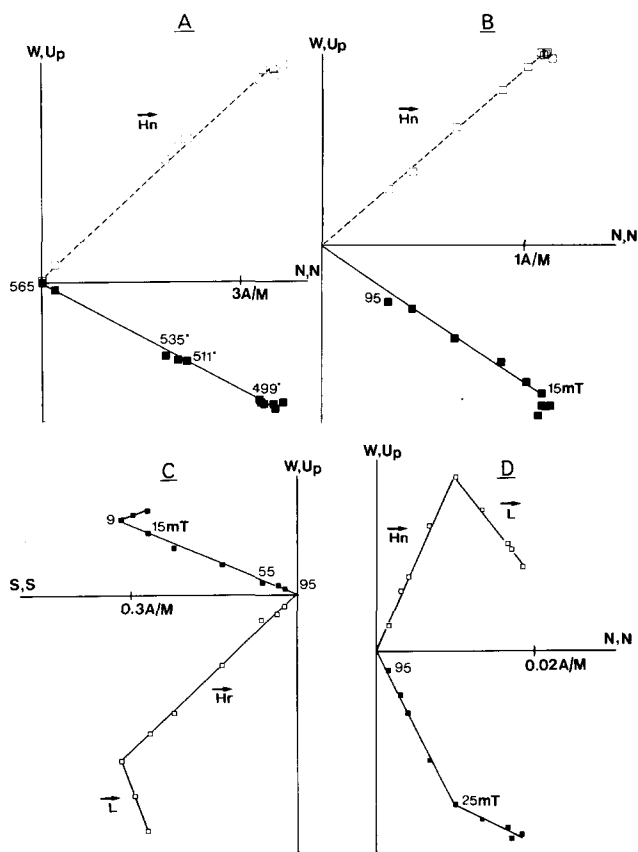


**Fig. 3.** Typical examples of thermal (A) and AF demagnetization (B–D) for samples from the Honningsvåg igneous complex. In orthogonal vector projections open (solid) symbols refer to points in the vertical (horizontal) plane. Label Hn (Hr) refer to high temperature/coercivity unblocking components of normal (reverse) polarity. Label L denotes low-unblocking components.

Petrographic studies identify magnetite (up to 50  $\mu\text{m}$  in length) as the dominant opaque phase, but it is of secondary origin and commonly formed by precipitation along grain boundaries or within microcracks. Small amounts of pyrrhotite (up to 100  $\mu\text{m}$  in length) were also observed.

Subordinate larger grains (up to 350  $\mu\text{m}$  in length) are weakly anisotropic, with more strongly anisotropic lamellae structures, and interpreted as hemo-ilmenite with lamellae of ilmenite or rutile. The lamellae post-date brittle (? D2) microcracking of the grains, and are restricted to sub-grain regions defined by the microcracking process.

### Magnetic fabrics

The anisotropy of magnetic susceptibility (AMS) was measured with a modified Minisep Delineator system, calibrated against a KLY-2 Kappabridge (University of Bergen). The ellipsoids of the anisotropy of isothermal remanent magnetization (AIRM) was also routinely determined (Table 3) from measurements of a low-field IRM (5 mT) induced in three orthogonal axes ( $X$ ,  $Y$  and  $Z$ ) after AF demagnetization in a field of 10 mT (Stephenson *et al.* 1986).

**Table 2.** Characteristic remanence components

Site	Comp	Dec	Inc	N	$\alpha^{95}$	k	Field/Temp
1	H	031	-30	14	3.5	130.3	>95 mT, 580°C
2	H	209	+49	14	5.8	47.2	>95 mT, 535°C
3	H	047	-39	14	7.0	33.5	>95 mT, 565°C
	L	019	+38	3	22.7	30.6	30 mT, 500°C
4	H	044	-29	15	4.8	64.0	>95 mT, 580°C
	L	030	+62	5	32.7	6.4	15 mT, 500°C
5	H	052	-47	26	2.8	105.1	580°C
	L	059	+52	13	10.4	16.8	500°C
6	—	—	—	—	—	—	—
7	H	056	-42	8	10.5	28.5	>95 mT, 550°C
8	H	057	-32	23	3.1	96.2	>95 mT, 570°C
	L	012	+70	9	13.8	15.0	20 mT, 400°C
9	H	028	-26	19	5.3	41.3	>95 mT, 580°C
	L	23	+61	3	25.7	24.1	4 mT, 510°C
10	H	061	-38	9	10.5	25.0	>95 mT, 580°C
<b>Site-mean statistics (in-situ)</b>							
	H <sup>N</sup>	046	-36	8*	8.5	43	VGP: N06, E343
	H <sup>R</sup>	209	+49	14	5.8	47.2	VGP: N13, E000
	H <sup>C</sup>	045	-38	9*	8.4	38.6	VGP: N07, E344 (6/10)
	L	030	+58	5*	15.1	26.5	VGP: N54, E164 (16/22)
<b>Specimen statistics (in-situ):</b>							
	H	045	-38	142	2.7	20.5	VGP: N07, E344 (2/3)
	L	037	+58	34	8.2	9.9	VGP: N53, E155 (9/12)

Comp, component; H, high blocking; L, low blocking; k, precision parameter (Fisher 1953); Field/Temp, maximum field/temperature range; VGP, virtual geomagnetic pole; dp/dm in parentheses. N, normal polarity; R, reverse polarity; C, combined polarity.

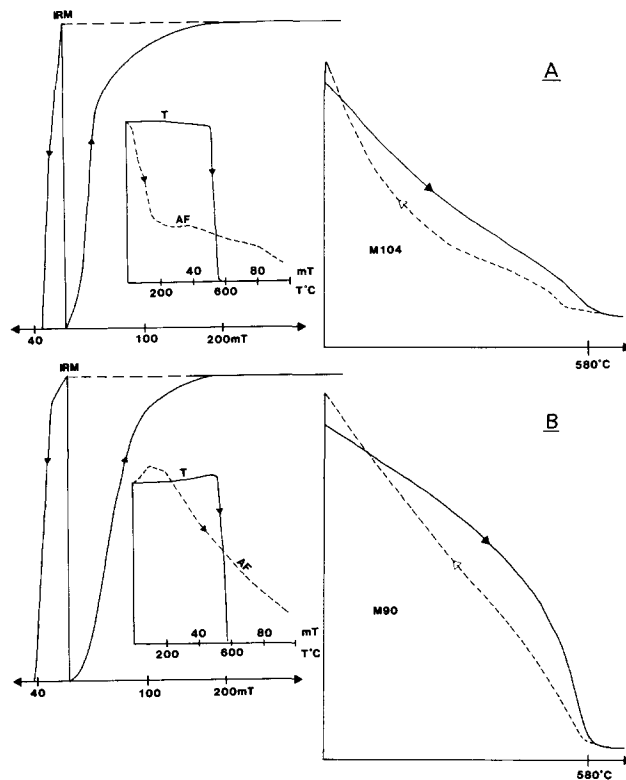


**Fig. 4.** Examples of isothermal remanence acquisition curves, AF and thermal unblocking spectra (inset diagrams with decay curves marked AF and T respectively) and thermo-magnetic curves for a sample from sites 9 (A) and 8 (B).

**Table 3.** Anisotropy of magnetic susceptibility (AMS) and remanence (AIRM)

Site	Eigenvalues			Eigenvectors		
	MAX e1	INT e2	MIN e3	MAX Dec/Inc	INT Dec/Inc	MIN Dec/Inc
1 AIRM	1.2027	1.0133	0.7834	198/50	046/35	307/13
AMS	1.0085	0.9937	0.9883	164/66	011/15	281/7
2 AIRM	1.3085	0.9565	0.7343	240/75	063/15	153/0
AMS	1.1434	1.0158	0.9421	283/80	032/3	123/9
3 AIRM	1.1587	0.9722	0.8683	—/—	—/—	—/—*
AMS	1.0196	1.0071	0.9879	245/36	028/46	142/19
4 AIRM	1.2930	1.1162	0.5901	224/6	118/69	318/18
AMS	1.0158	0.9960	0.8669	084/40	212/36	326/28
5 AIRM	1.2795	1.0465	0.6731	092/52	245/36	346/9
AMS	1.1583	1.1149	0.9453	094/55	259/33	354/7
6 AIRM	1.3105	1.1310	0.5580	312/78	082/8	174/7
AMS	1.0582	0.9788	0.9021	356/76	097/2	188/13
7 AIRM	1.2270	0.9985	0.7733	141/56	286/27	019/13
AMS	1.0658	0.9776	0.9533	104/41	254/44	001/15
8 AIRM	1.3185	0.9446	0.7364	191/62	333/24	070/17
AMS	1.0945	1.0302	0.9325	217/58	320/7	55/31
9 AIRM	1.1342	0.9818	0.8831	—/—	—/—	—/—*
AMS	1.0935	1.0484	0.9631	—/—	—/—	—/—*
10 AIRM	1.0822	1.0034	0.9133	—/—	—/—	—/—*
AMS	1.0718	0.9884	0.9341	—/—	—/—	—/—*

MAX, INT & MIN, maximum, intermediate & minimum axes of the triaxial susceptibility ellipsoid; Dec/Inc = mean declination/inclination for the principal axes.

\*Not directionally consistent at site-level.

**Eigenvalues**

The AMS eigenvalue ratio, P2 ( $K_{max}/K_{min}$ ), varied from 1.02 to 1.22, whereas AIRM P2 values proved an order of magnitude higher, ranging from 1.18 to 2.44 (Fig. 5A). The shapes of the AIRM and AMS ellipsoids commonly differ, and P2 and eigenvalue-ratios of AMS and AIRM proved unrelated (Fig. 5B). This suggests that AMS and AIRM originate from different mineral sources; it is inferred that the AIRM is governed by magnetite whilst the AMS is mostly influenced by the anisotropy of dia- and paramagnetic mineral phases and/or hemo-ilmenite.

**Eigenvectors**

All sites, except sites 9 and 10, exhibit well-defined within-site directionally consistent AMS magnetic foliation planes ( $K_{max}-K_{int}$ ) and lineations ( $K_{max}$ ). The AMS magnetic foliation planes (/lineations) are steeply inclined (59–90°) and coincide with cumulate layering when this is observed in the field (e.g. site 1). In many cases cumulate layering is difficult to observe, and the internal structure of the Honningsvåg igneous complex is better depicted by the AMS magnetic foliation planes.

Along the western margin of the complex, the AMS magnetic foliation planes strike NNE, parallel to the structure observed in the immediate metasedimentary envelope, but toward the south east they show a consistent clockwise rotation (Fig. 6A). AMS and AIRM eigenvectors are closely similar, hence the ‘structural’ arc or reclined fold as recognized from the AMS data is also discerned from the AIRM data (compare Figs 6A & B).

**Characteristic remanence data: structural considerations**

Specimen and site-level distributions of high temperature/coercivity unblocking (H) and low temperature/coercivity (L) components are portrayed in Fig. 7. Component L probably represents a Mesozoic overprint direction and is not considered further here.

Component H is well grouped with a subordinate declination smearing (cf. Figs 6C & 7) related to the structural arc defined by the anisotropy & magnetic susceptibility and isothermal remanent magnetization data (Fig. 6A & B). Site-mean declinations and AMS foliation strike-trends show a correlation coefficient (R) of 0.82 (Fig. 6D). Such a relationship could either have a structural origin or relate to thermoremanent magnetization (TRM) deviation. The latter explanation relates to the acquisition of secondary TRM in an anisotropic rock. TRM deviation can theoretically be corrected by remanence destaining using the AIRM data since their eigenvalues are broadly similar to those of anisotropy of TRM (Stephenson *et al.* 1986). However, TRM deviation analysis introduces increased directional scatter (see methods in Stephenson *et al.* 1986, Cogne 1988 and Torsvik *et al.* 1990); hence TRM deviation fails to explain the directional relationship between remanence and fabrics (Fig. 8A). Similarly, stepwise unfolding, using AMS foliation planes, gives increased directional scatter (Fig. 8B). Thus, component H is

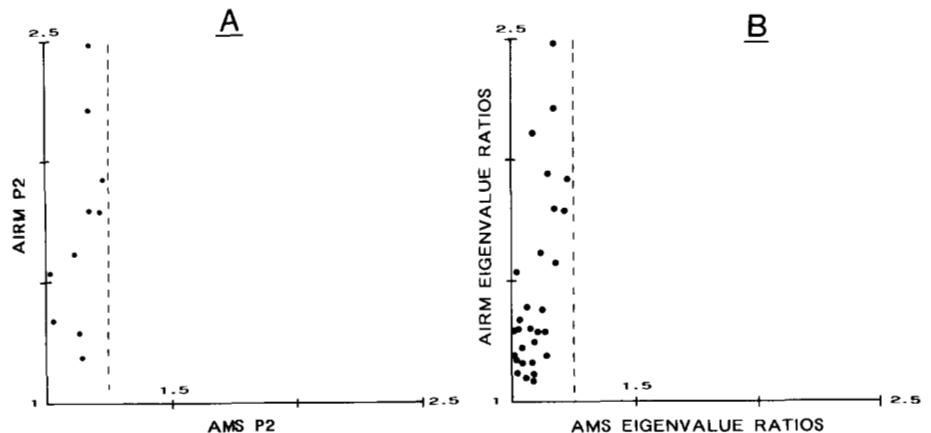
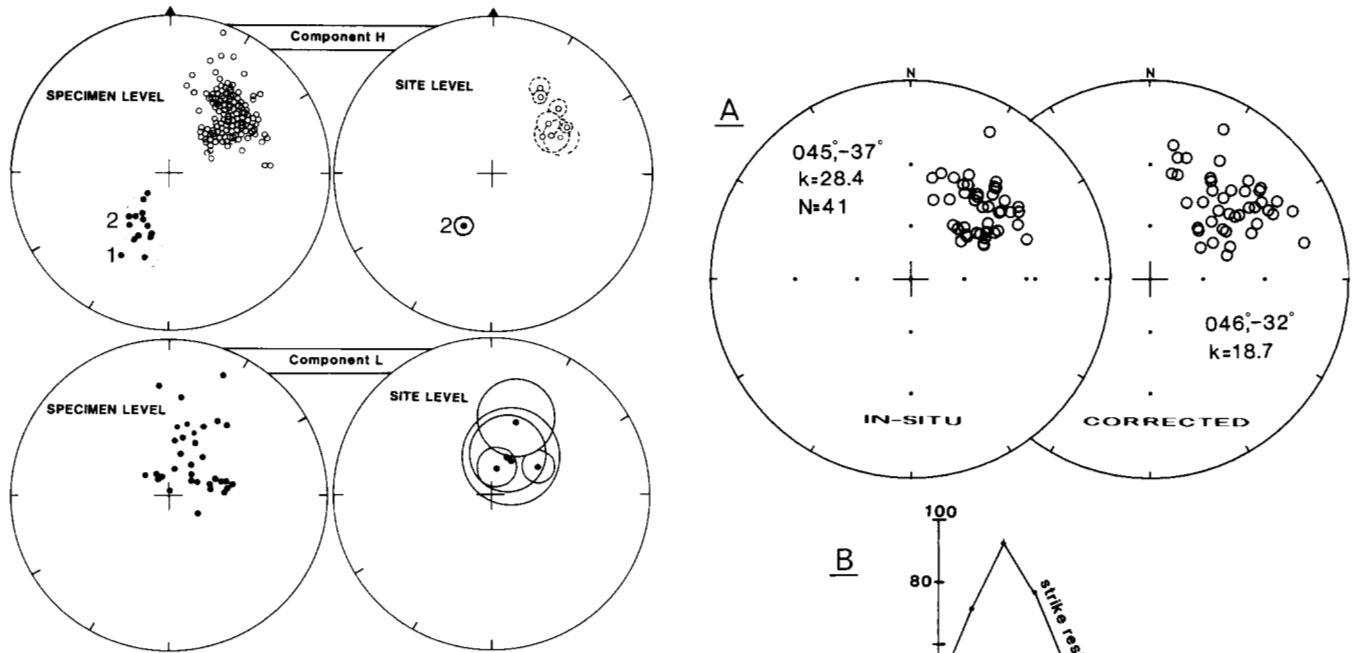
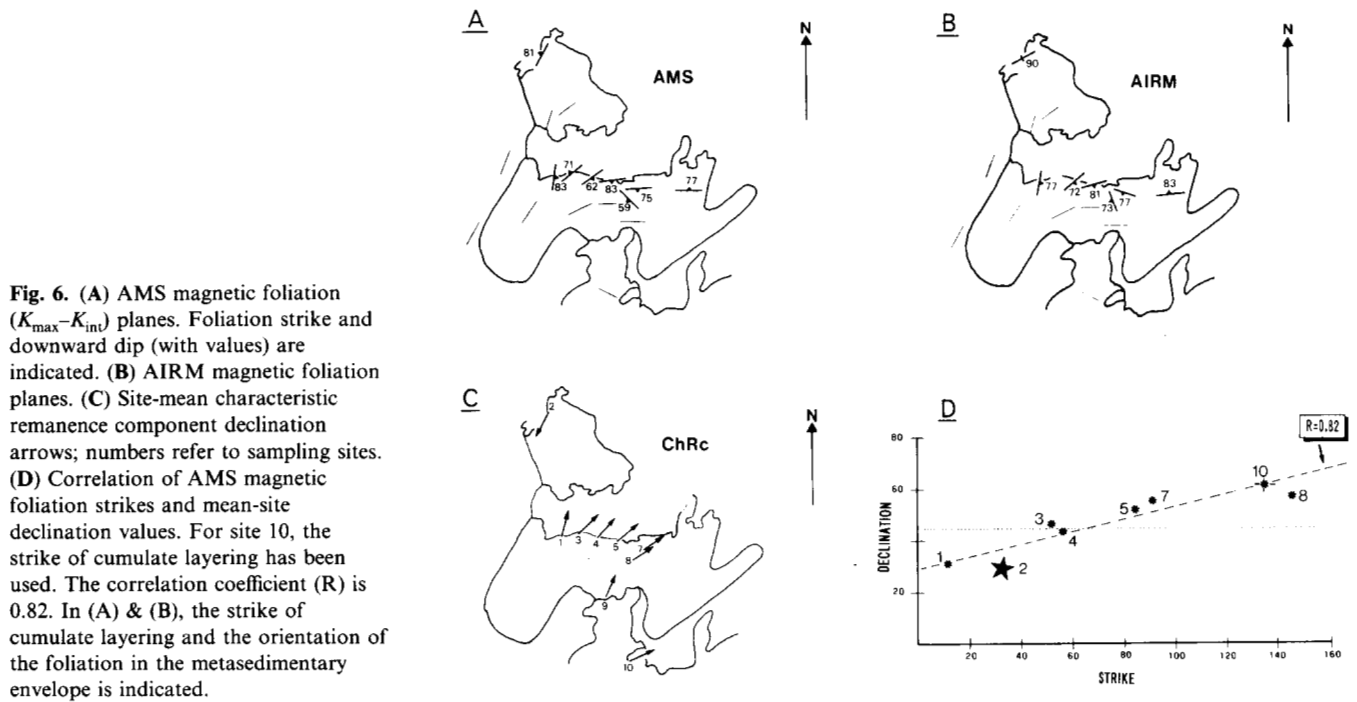


**Fig. 5.** (A) Comparison of anisotropy of magnetic susceptibility (AMS) and anisotropy of isothermal remanent magnetization (AIRM) P2 ( $K_{max}/K_{min}$ ) eigenvalue ratios. (B) Comparison of AMS and AIRM P1 ( $K_{max}/K_{int}$ ), P2 and P3 ( $K_{int}/K_{min}$ ) eigenvalue ratios. Notice the lack of correlation.



clearly of post-fold origin, given the assumption that the gabbroic cumulate layering was originally horizontal (top to the SE).

Conversely, remanence 'dispersion' is reduced by a *partial* structural strike restoration (Fig. 8b). Strike restoration, using

Fig. 8. (A) TRM deviation analysis. Note the increased scatter after correcting for possible effects of TRM deviation. (B) Stepwise unfolding using AMS magnetic foliation planes which closely compares with the cumulate layering, and stepwise strike restoration using AMS magnetic foliation strikes.

AMS foliation planes and retaining site 4 as an arbitrary fixed reference direction, shows optimal remanence grouping at 20 percent strike restoration. It is therefore likely that the declination dispersion, though small, relates to folding of a pre-existing structure (?D1), or alternatively that component H is syn-tectonic with respect to either D1 or D2. The overall effect on the mean declination of this proposed folding, is comparably small, and so there is reasonable confidence in the palaeomagnetic validity of the reported in-situ mean directions (Table 2).

### Potential field data

The magnetic data from the investigated area were collected on an airborne survey, flight altitude 750 m, with a line-spacing of 2 km (Norges Geologiske Undersøkelse 1972). The gravity

data are based on *c.* 200 gravity observations (Fig. 9A), mainly measured by Lønne & Sellevoll (1975). Both data-sets were subsequently gridded (500 × 500 m) and contoured (Fig. 9) at the Geological Survey of Norway. Additionally, gridded topographic data (100 × 100 m), made available by the Norwegian Mapping Authorities, were examined. These grid-sets were subsequently analyzed on an ERDAS image processing system (Erdas 1990). All three raster data-sets were processed simultaneously allowing detailed comparison and rapid analyses. Histogram-equalized colour, high-frequency filtering and shaded-relief image techniques were used to enhance the original datasets (Henkel *et al.* 1984; Gonzales & Wintz 1987, Lee *et al.* 1990). Only the topographic data proved valuable for lineament analysis, and hence gravity and magnetic data are presented as ordinary contoured maps with 20 g.u. and 20 nT line intervals (Fig. 9).

Petrophysical properties from the Honningsvåg igneous complex are listed (Table 1) and the surrounding metasedimentary properties are given by Olesen *et al.* (1990). The induced/remanent contribution from the metasedimentary rocks is small and has been ignored in magnetic modelling. A density contrast of 0.20 Mg/m<sup>3</sup> between the Honningsvåg igneous complex (2.93) and the metasedimentary envelope (2.73) was employed (Lønne & Sellevoll 1975, Olesen *et al.* 1990) in gravity modelling. Modelling parameters are listed in Table 4.

### Modelling

Eight magnetic, gravity and topographic profiles were extracted from the grid data-sets (Fig. 1) for 2½ dimensional forward modelling (Software developed by T.H.T. after theory (algorithms) outlined in Shuey & Pasquale 1973, Rasmussen & Pedersen 1979 and Enmark 1981).

The Magerøy area is associated with a positive, *c.* 15 km wavelength, Bouguer gravity anomaly, reaching a maximum of *c.* 250 g.u. over the central parts of the complex (Fig. 9A, Profile 7). The residual gravity anomaly for Profile 7 (linear background field correction), together with a likely geological model (see later) to explain the observed gravity anomaly is portrayed in Fig. 10A. In this model, the complex extends to a depth of *c.* 6 km with overall NW dip of the order of 60–80°. The model is in overall agreement with the gravity interpretation of Lønne & Sellevoll (1975).

The aeromagnetic signature of the Honningsvåg igneous complex is intriguing. Apart from a *c.* 3 km short-wavelength positive anomaly of 700 nT, located a few kilometres NW of the gravity maximum (Kamøyvær), the aeromagnetic signature of the HIC is dominated by a long-wave (> 50 km) regional negative anomaly (Fig. 9B). It becomes evident that the aeromagnetic signature of the complex is influenced by the remanent properties, and most notably by the magnetic polarity pattern. Indeed, the remanent magnetization for normal polarity sites (NE and up), which dominate the complex (8 of 10 sites), obliterates the induced field-component or produces a minor negative anomaly (Fig. 10B & C). Conversely, the positive anomaly located at Kamøyvær is situated above a region of reverse remanent polarity (site 2) and in this case a component of the remanent vector augments the induced field. The bulk-susceptibility is also notably higher from this site (Table 1), thereby enhancing the induced component (Fig. 10B & C).

The presented model anomalies simulate the aeromagnetic and gravity observations (Fig. 10). The depth and shape of the Honningsvåg igneous complex are essentially constrained by

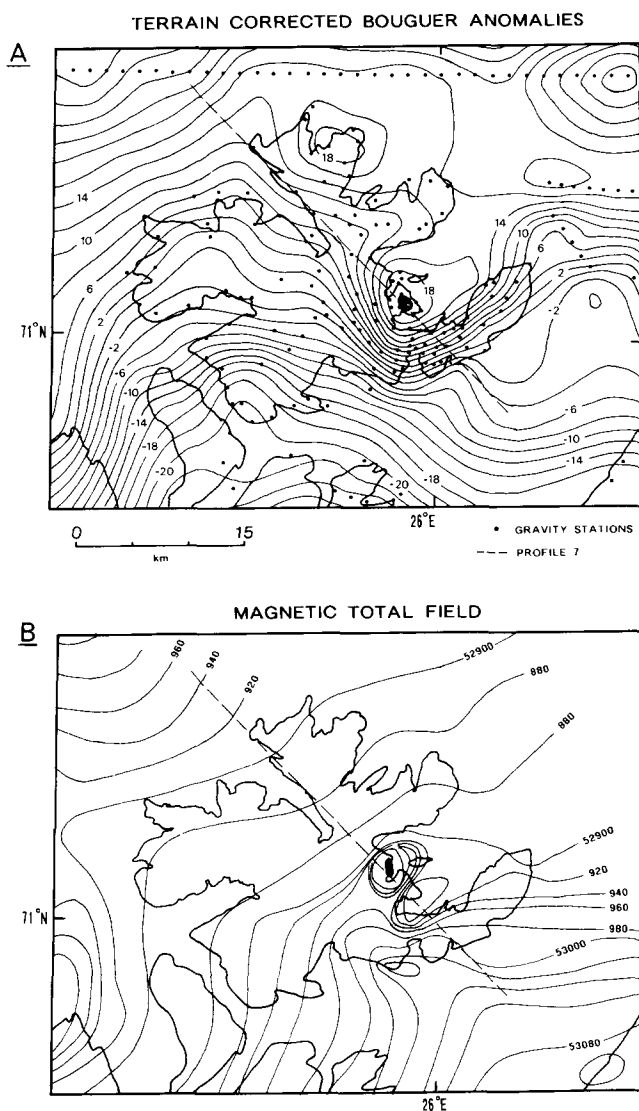


Fig. 9. (A) Contoured Bouguer anomaly map (contours in g.u. × 10 at 20 g.u. intervals) (B) Contoured magnetic total field map (20 nT interval) Gravity (> 200 g.u.) and magnetic maxima (> 53 500 nT) are shaded. Dashed line refers to profile 7 (see Fig. 1).

**Table 4.** Magnetic and gravity modelling parameters (see Fig. 10)

Body	P	SUS ( $10^{-6}$ SI)	DEC	INC	NRM(mA/M)	Y(km)	DC(g/cm <sup>3</sup> )
1	R	10441 (40 000)*	215	+57	2000 (566)*	4.0	+0.20
2	N Main	3148	049	-26	680	4.0	+0.20
3	N East	3148	049	-26	450	5.0	+0.20

P, Palaeomagnetic polarity; DC, density contrast; Y, half-width of body used in magnetic and gravity model.

Regional Earth's Magnetic Field Dec/Inc:  $6^{\circ}/79^{\circ}$

Regional Earth's Magnetic Field Intensity: 53125 gamma

\*Alternative model for Body 1 with increased susceptibility (see text).

the gravity data. The gravity model is sensitive to small changes in width and length along strike, and the model has been divided in two parts. Part I includes bodies 1 and 2 with a total width of 4 km and part II consists of body 3 with a width of 5 km. On the other hand, the magnetic model is internally constrained by the areas of normal and reverse polarity (Fig. 10B), but the external shape and widths match the gravity model (Fig. 10A). The magnetic data require a thin and near vertical body with reverse polarity magnetization to explain the observed anomaly; the model is *not* strongly depth-sensitive and the depth extent of the reverse polarity body can be substantially reduced by increasing the bulk-susceptibility and/or remanent intensity parameters for the body. The

observed surface intensity or susceptibility at site 2 is too low to explain the observed anomaly, irrespective of the depth of body 1, and indeed depths corresponding to the Curie-temperature isotherm for magnetite, say 20 km, can only explain half of the observed anomaly. This can be resolved by (1) increasing the susceptibility of the body to 40 000 ( $10^{-6}$  SI), (2) increasing the remanent intensity to 2000 mA/m, or (3) increasing both petro-physical parameters. The susceptibility required for alternative (1) is unlikely, and exceeds the maximum susceptibility range recorded from the complex. Conversely, an average remanent intensity of 2000 mA/m falls within the range recorded from other sampling sites in the complex (e.g. site 1).

### Concluding remarks

The palaeomagnetic signature of the Honningsvåg igneous complex is dominated by a secondary magnetite-bearing and *dual-polarity* high-unblocking temperature/coercivity component (**H**). A subordinate lower stable remanent component, probably early Mesozoic (? Triassic) in age, was also identified. Compared with relevant palaeomagnetic data from Baltica (Torsvik *et al.* 1990), a Siluro-Devonian (Scandian) age is indicated for the **H** component.

Structural and microfabric data demonstrate that the complex has been tilted through  $90^{\circ}$ , probably during late D1 age (Andersen 1981), and straightforward gravity modelling suggests that the tilted complex extends to a depth of *c.* 6 km and constitutes a steeply inclined body with margins nearly parallel to the cumulate layering. Conversely, magnetic modelling is complex since the contribution of remanent magnetization to the total-field anomaly is considerable. Indeed, the dual-polarity NRM pattern controls the aeromagnetic signature in the area, and a pronounced magnetic anomaly of *c.* 700 nT coincides with an area dominated by reverse palaeomagnetic remanence polarity. In these circumstances, magnetic modelling requires strong petrophysical control, including detailed knowledge of remanence direction and intensity.

While the external shape of the Honningsvåg igneous complex can be modelled by the potential field data, the AMS and AIRM data delineate its internal structure. These micro-fabric data identify a structural arc or reclined fold within the complex, and it is further substantiated that there is a partial relationship between the structural strike and the remanent declinations (component **H**). Taken at face value, the magnetization age is consequently syn-tectonic with respect to the Scandian orogenic event, probably acquired from post-D1 uplift and subordinately modified/dispersed by D2 deformation. This remanence acquisition model requires that D2 deformation took place under brittle upper-crust conditions without marked tectonothermal magnetic resetting.

Biostratigraphical and structural considerations imply a

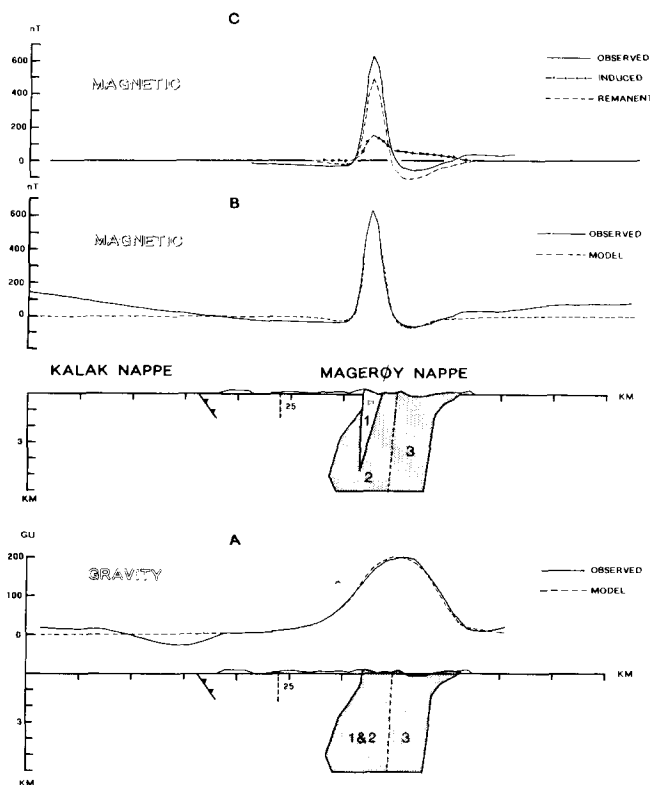


**Fig. 10.** 2½ dimensional forward modelling using Profile 7 (see location in Figs 1A and 9). Model properties are listed in Table 4. In the top diagram (C), the induced and remanent contributions to the magnetic model are shown separately. In (B) body 1 is of reverse palaeomagnetic polarity, whereas bodies 2 & 3 are of normal polarity (see Table 4).

post-Llandovery (<425 Ma) maximum remanence age, whereas isotopic data signify a minimum age of earliest Devonian (D2), c. 410 Ma (Anderson *et al.* 1982). Based on isotopic data from the Gjesvær migmatites (410 ± 28 Ma), but more importantly the syn-tectonic Finnvik Granite (Fig. 1a), which intruded between D1 and D2 (Rb-Sr whole rock ages; Andersen *et al.* 1982), an age of 411 ± 7 is inferred for the H component.

The pole-position of component H plots along the Late Silurian–Early Devonian apparent polar wander path for Baltica (Torsvik *et al.* 1990; Trench & Torsvik 1991). This, along with structural considerations and isotopic data from the Finnvik Granite, implies that the Cambrian–Early Ordovician ages reported by Krill *et al.* (1989) should be treated with extreme caution. The Honningsvåg igneous complex pole statistically overlaps with a Scandian pole reported from the underlying Finnmarkian Kalak nappe complex (Torsvik *et al.* 1990, Pole A). Hence, both isotopic (Andersen *et al.* 1982; Dallmeyer 1988) and palaeomagnetic evidence show that Scandian emplacement of the Magerøy nappe was associated with considerable tectonothermal resetting in the underlying Kalak nappe complex.

We thank the Norwegian Research Council for Science and the Humanities, the Geological Survey of Norway and the Natural Environment Research Council for financial support. D. Roberts, B. A. Sturt, B. Dahlø and two anonymous referees provided critical reviews. Norwegian International Lithosphere Project contribution (130).

## References

- AITCHESON, S. J., DALY, J. S. & CLIFF, R. A. 1989. A late Proterozoic orogen in the North Norwegian Caledonides. *Terra Abstracts*, **1**, 15.
- ANDERSEN, T. B. 1981. The structure of the Magerøy Nappe, Finnmark, North Norway. *Norges Geologiske Undersøkelse Bulletin*, **363**, 1–23.
- 1989. A comment: Alternative to the Finnmarkian-Scandian interpretation on Magerøya, northern Norway. *Norsk Geologisk Tidsskrift*, **69**, 291–294.
- AUSTRHEIM, H., STURT, B. A., PEDERSEN, S. & KJÆRSRUD, K. 1982. Rb-Sr whole rock ages from Magerøy, North Norwegian Caledonides. *Norsk Geologisk Tidsskrift*, **62**, 79–85.
- COGNE, J. P. 1988. Strain-induced AMS in the granite of Flamanville and its effects upon TRM acquisition. *Geophysical Journal*, **92**, 445–453.
- CURRY, C. J., 1975. *A regional study of the geology of the Magerøy basic igneous complex and its envelope*. PhD thesis, University of Dundee.
- DALLMEYER, R. D., 1988. Polyorogenic <sup>40</sup>Ar/<sup>39</sup>Ar mineral age recorded within the Kalak Nappe Complex, Northern Scandinavian Caledonides. *Journal of the Geological Society, London*, **145**, 705–716.
- DALY, J. S., AITCHESON, S. J., CLIFF, R. A., GAYER, R. A. & RICE, A. H. N. 1991. Geochronological evidence from discordant plutons for a late Proterozoic orogen in the Caledonides of Finnmark, northern Norway. *Journal of the Geological Society London*, **148**, 29–40.
- ENMARK, T. 1981. A versatile interactive computer program for computation and automatic optimization of gravity models. *Geoexploration*, **19**, 47–66.
- ERDAS, 1990. *Image processing module, version 7.4, January 1990*. Erdas Inc., Atlanta, USA.
- FISHER R. A. 1953. *Dispersion on a sphere*. Proceedings of the Royal Society, London, **A217**, 295–305.
- GONZALES, R. C. & WINTZ, P., 1987. *Digital image processing*. Addison-Wesley Publishing Company, Reading, Massachusetts, USA.
- HENKEL, H., AARO, S., HULTSTRØM, J., KERO, L., MELLANDER, H. & ANDERSSON, C. 1984. *Filipstadprosjektet—en test av bilde-behandlingsystemet EBBA-1 for regionala geofysiske data*. SGU Geophysical Report **8408**.
- KRILL, A., A. G., RODGERS, J. & SUNDVOLL, B., 1989. Alternative to the Finnmarkian-Scandian interpretation on Magerøya, Northern Norway. *Norsk Geologisk Tidsskrift*, **68**, 171–185.
- LEE, M. K., PHARAOH, T. C. & SOPER, N. J. 1990. Structural trends in central Britain from images of gravity and aeromagnetic fields. *Journal Geological Society, London*, **147**, 241–258.
- LØNNE, W. & SELLEVOLL, M. A. 1975. A reconnaissance gravity survey of Magerøy, Finnmark, Northern Norway. *Norges Geologiske Undersøkelse Bulletin*, **319**, 1–15.
- NORGES GEOLOGISKE UNDERSØKELSE 1972. *Aeromagnetic map Nordkapp 1:250,000*.
- OLESEN, O., ROBERTS, D., HENKEL, H., LILE, O. B. & TORSVIK, T. H. 1990. Aeromagnetic and gravimetric interpretation of regional structural features in the Caledonides of West Finnmark and North Troms, northern Norway. *Norges Geologiske Undersøkelse Bulletin*, **419**, 1–24.
- PEDERSEN, R. B., DUNNING, G. R. & ROBINS, B., 1989. U-Pb ages of nepheline syenite pegmatites from the Seiland magmatic province, N. Norway. In: GAYER, R. A. (ed.) *The Caledonide Geology of Scandinavia*. Graham & Trotham, London, 3–8.
- RAMSAY, D. M. & STURT, B. A. 1976. The syn-metamorphic emplacement of the Magerøy Nappe. *Norges Geologiske Tidsskrift*, **56**, 291–307.
- RASMUSSEN, R. & PEDERSEN, L. B. 1979. End corrections in potential field modeling. *Geophysical Prospecting*, **27**, 749–760.
- ROBERTS, D. & ANDERSEN, T. B. 1985. Nordkapp. Description of the 1:250,000 geological map. *Norges Geologiske Undersøkelse Skrifter*, **61**, 1–49.
- ROBINS, B. 1990. *Skarsvåg. Bedrock map 2137(3)—1:50,000, preliminary version*. Norges Geologiske Undersøkelse.
- , HAUKVIK, L. & JANSEN, S., 1987. The organization and internal structure of cyclic units in the Honningsvåg intrusive suite, North Norway: Implications for intrusive mechanisms, double-diffusive convection and pore-magma infiltration. In: PARSONS, I. (ed.) *Origins of Igneous Layering*. D. Reidel Publishing Company, 287–312.
- SHUEY, R. T. & PASQUALE, A. 1973. End corrections in magnetic profile interpretation. *Geophysics*, **38**, 507–512.
- STEPHENSON, A., SADIKUN, S. & POTTER, D. K. 1986. A theoretical and experimental comparison of the anisotropies of magnetic susceptibility and remanence in rocks and minerals. *Geophysical Journal of the Astronomical Society*, **84**, 185–200.
- STURT, B. A., PRINGLE, I. R. & ROBERTS, D. 1975. Caledonian nappe sequences of Finnmark, northern Norway, and the timing of orogenic deformation and metamorphism. *Geological Society of America Bulletin*, **86**, 710–718.
- & RAMSAY, D. M. 1978. The Finnmarkian phase of the Caledonian Orogeny. *Journal of the Geological Society, London*, **135**, 597–610.
- TORSVIK, T. H., OLESEN, O., RYAN, P. D. & TRENCH, A., 1990. On the palaeogeography of Baltica during the Palaeozoic: new palaeomagnetic data from the Scandinavian Caledonides. *Geophysical Journal International*, **103**, 261–279.
- , RYAN, P. D., TRENCH, A. & HARPER, D. H. T. 1991. Cambrian-Ordovician palaeogeography of Baltica. *Geology*, **19**, 7–10.
- TRENCH, A. & TORSVIK, T. H. 1991. The Lower Palaeozoic Apparent Polar wander path for Baltica: Palaeomagnetic data from Silurian Limestones of Gotland, Sweden. *Geophysical Journal International*, **107**, 373–379.